World Applied Sciences Journal 21 (4): 526-535, 2013
ISSN 1818-4952

DOI: 10.5829/idosi.wasj.2013.21.4.2270

Investigation of Loading Parameters in Detection of Internal Cracks of Composite Material with Digital Shearography

Davood Akbari and Naser Soltani

School of Mechanical Engineering, College of Engineering, University of Tehran, Iran

Abstract: Laser shearography is a speckle interferometric technique for full-field measurement of surface displacement derivatives. This technique has proved highly effective for nondestructive testing (NDT) of many kinds of material, especially composites. The key to the success of shearography as a NDT method is to impose an appropriate stress status on the object under test. In this paper mechanical loading for detection of artificial cracks in glass fiber reinforced composites is investigated. In this regard, a dimensionless parameter named "load ratio" or "LR" is defined to present the loading status in the elastic region. Crack-type defects were simulated by cutting several grooves with different sizes and orientations in an 8layer fiber reinforced composite plate. The tests have been performed with different "LR"s to evaluate the capability of shearography in detection of the cracks and to extract the proper ranges of load ratio from the test results. It has been showed that the load ratio is an important parameter in the inspection procedure beside other parameters like shearing distance and direction. The effects of the shearing and crack direction in the defect detection capability of the shearography system have also been investigated.

Key words: Nondestructive testing · Digital shearography · Internal Crack · Mechanical loading

INTRODUCTION

Composite materials have received a great deal of consideration for structural applications, because of their high strength to weight ratio. Though, the risk of existence of different flaws in these kinds of material is generally higher than that in metals, because they made of combination of two or more materials glued together. These undesirable defects affect the structure and its mechanical properties, so in order to check the integrity of the structure, these defects have to be revealed. Consequently, there is a need to monitor defects in composite structures during and after fabrication and also in service. In the other hand, many limitations like being inhomogeneous, anisotropic, nonconductive and nonmagnetic make many conventional Non-Destructive Testing (NDT) methods inapplicable in composite materials. Therefore, there is a need to develop new and robust testing techniques which will detect defects of this type quickly and reliably.

In recent years, the non-destructive evaluation (NDE) of materials and structures have benefited from development of optical full field methods and their nature of being full-field, non-contacting and non-contaminating [1]. Moreover the results of the inspection are images that give visual representations of the condition of the components. Infra-Red Thermography [2], holography [3], Electronic Speckle Pattern Interferometry (ESPI) [4] and shearography [5] are some kinds of optical-based NDT methods. Among these methods, Shearography (as called Speckle Pattern Shearing Interferometry) has been developed as an important technique in NDT due to its advantages over the related techniques of holography and ESPI. Shearography directly measures the derivatives of displacement and it has reduced coherence requirements and sensitivity to vibration due to its use of an almost common-path interferometer [6].

As a NDT technique, shearography reveals defects within an object by identifying defect-induced deformation anomalies when the object is loaded. Successful application of shearography for NDT is strongly dependent on the type and magnitude of the loading and also the set-up parameters like shearing distance. The most common loading methods used to

Corresponding Author: Davood Akbari, Mechanical Engineering group, Faculty of Mechanical Engineering, Tehran University, Tehran, Iran. Tel: +98 21 61114055

reveal different kinds of defects in the test parts are pressurizing, partial vacuum, mechanical loading, thermal and vibration excitation.

The most common kinds of defects in composite structures that are identified using shearography method include delamination, disbonding and wrinkles. Hung [7] reviewed the use of shearography for nondestructive evaluation of composite structures including debond in composite laminates, delamination in composite honeycomb panels, etc. Toh *et al*. [8] applied vacuum stressing method to illustrate the application of shearography for estimating the size and depth of disbonds in glassfibre reinforced plates. They show that disbonds in an objects can be sized from the boundaries of the anomalous fringe patterns and their depths can be estimated from the number of fringes appeared within the defective areas. Garnier *et al.* [9] evaluate the efficiency of three NDT methods (Ultrasonic, Thermography and Shearography) in the detection of delaminations resulting from Impact Damages or in-service damages. They concluded that only the ultrasonic method enables the depth of a defect but it appears that Infrared Thermography and Shearography produced results very quickly compared to Ultrasonic Testing. DeAngelis *et al.* [10] used vibration dynamic loading to reveal flat bottom holes indicating disbounds in CFRP laminates with different sizes. They evaluated the flaw detection capabilities of shearography by measuring dynamic response of defects to applied stresses by a proposed numerical-experimental procedure.

Liu *et al.* [11] investigated the capabilities of shearography for detecting hole and crack type defects in polymeric and metallic materials using thermal loading. They showed that in metals and polymers, for those defects having a larger ratio of length to width such as cracks and grooves, the detection becomes difficult if the shearing direction hasn't been set properly. Schöntag *et al.* [12] presented an investigation on the applicability of shearography to characterize the location and depth of defects in composite materials. In this work they used sets of specimens with artificial square flaws between the layers of a composite material for the experiments. Time-Average and Stroboscopic laser illumination have been applied together with vibrational loading. They characterized the depth of defects by relating the resonance frequencies of the objects to the depths of the different faults sizes. Celine *et al.* [13] demonstrated an experimental technique for fringe analysis of sub-surface defects using variance of directly fringe-shifted shearograms. They mentioned that this statistical technique has the advantage of being robust against speckle noise compared to other methods of defect localization. Guo *et al.* [14] presented a method for inspection of kissing-bond defects of sandwich plates. A laser shearography system with vacuum loading device was used for inspection of a sandwich structure test panel with artificial defects. In this work, they used finite element analysis for deformation calculation at the surface of defects with different vacuum loads.

Most of the investigations in shearography NDT of composite materials have been focused on delamination and disbonding as they can be easily detected by shearography. Thermal loading and partial vacuum are common methods of excitation to detect disbonds in composite structures, but these loading methods cannot be properly applied to detect crack-shaped defects. However, the thermal loading leads to the results that can be affected by non-uniform heating load. This leads to an irregular background which masks the defect localization [15]. Moreover, the defect-induced changes of fringe pattern can be much smaller than background noise signal. In addition, partial vacuum needs special equipment that makes this method laborious in the real inspection. However there are very limited researches about the loading characteristic and parameters in detecting internal cracks of composite laminates.

In this paper mechanical loading is investigated for detecting cracks in glass fiber reinforced composites. In this regard several test plates were prepared with deliberately made cracks, created with different sizes and orientations. Shearography NDT of the defected specimens was performed by applying tensile loading.

To evaluate the loading status in the shearography tests, a parameter named load ratio has been defined as the ratio of the average stress in the section of the test plate over the elastic modulus of the material. Because in the shearography tests, the required loading is almost applied in the elastic region, this dimensionless parameter can be properly used as a tool for determining the loading status. In each test, the visibility of the shearography results was evaluated respect to the applied load ratio and the best matching load for each crack size and orientation was obtained.

The measuring sensitivity of shearography depends on the wavelength of the laser and shearing distance. If the used laser has been determined, shearing distance has a major effect in the results of the shearography tests. So, the effects of the shearing

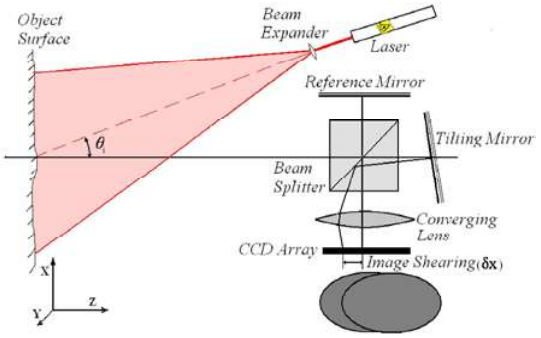

Fig. 1: Michelson-based interferometer set-up of digital shearography

distance were considered in the results of the shearography tests of this paper by adjusting different amounts of shear in the experiments.

Principles of Shearography

Fringe Formation: The main principle of shearography is to make a pair of laterally displaced, or sheared, speckle images. There are some optical devices that can be used to make a sheared image like: wedge plate [16], Savant polar scope [17], Wollaston prism [18], wedge prism [19] and modified Michelson based interferometer [10]. A typical optical setup of digital shearography based on modified Michelson interferometer is shown in Fig 1. The test object is illuminated by an expanded laser beam. When the light reflects from the surface of the object, it is focused on the image plane of the CCD-camera via two mirrors placed on two sides of the beam splitter. By turning one of the mirrors for a very small angle, a pair of laterally sheared images of the test object is generated on the CCD-camera. The shearing amount can be controlled by the tilting mirror.

The two sheared images interfere with each other producing a speckle pattern. After the object is stressed, the second speckle pattern is registered by the CCD-camera again and stored in another frame. Digital subtraction between these two recorded images forms a fringe pattern depicting displacement gradient of the tested surface.

The irradiance I(x,y) of the interference of two sheared images is given by [20]:

$$I(x, y) = 21_0(1 + \gamma\cos(\varphi(x, y))) \quad (1)$$

where I_0 represents the average intensity of the two sheared light waves, γ represents the modulation of the interference term and $\varphi(x, y)$ is the relative phase between the two sheared images. After the object is loaded or the load is changed, the object is deformed and the intensity distribution of the speckle pattern is slightly altered by I'(x, y), represented by Error! Reference source not found.:

$$I'(x, y) = 21_0[1 + \gamma\cos(\varphi'(x, y))] \quad (2)$$

where $\varphi'(x, y)$ is the relative phase of each speckle after deformation of the object. Subtraction of Eq 1. from Eq 2. yields:

$$I_s = I - I' = I_0[\gamma\cos\varphi - \gamma\cos(\varphi + \Delta)] = 21_0\gamma\sin(\varphi + \frac{\Delta}{2})\sin(\frac{\Delta}{2}) \quad (3)$$

where Δ describes the relative phase change $\Delta[\Delta = \varphi'(x, y) - \varphi(x, y)]$ occurring due to the object deformation. Eq 3. represents a fringe pattern that can be displayed on the monitor in real time (at video rate). From Eq 3. it is concluded that Dark fringes will appear in the subtracted images whenever $\Delta=2\pi N$, where N is an integer and bright fringes will appear in the subtracted image whenever $\Delta=\pi(2N+1)$. In this manner, dark and bright fringes can be sequentially numbered with integers.

Out of Plane Displacement Derivatives: It can be shown [5, 6, 20] that the relative phase change Δ is related to the displacement derivatives due to the shearing function of shearography. According to Fig 1. If the observation and illumination positions lie in the *x*, *z* plane and the imaging area of the object is small compared to the source to object and object to camera distances, the phase difference can be represented by [20]:

$$\Delta=\frac{2\pi}{\lambda}(\sin\theta\frac{\partial u}{\partial x} + (1+\cos\theta)\frac{\partial w}{\partial x})\delta x \quad (4)$$

where θ is the angle between the illumination and observation directions; ë is the illuminating light wavelength; u and w are the displacement components along the reference x-and z-axes, respectively and δx is the amount of shear directed along the x-axis; if the shearing direction lies in the y axis, Eq 4. changes to:

$$\Delta=\frac{2\pi}{\lambda}(\sin\theta\frac{\partial u}{\partial y} + (1+\cos\theta)\frac{\partial w}{\partial y})\delta y \quad (5)$$

where δy is the amount of shear along the y-axis.

By making the observation and illumination directions close to collinear, the term $\sin\theta$ in Eq 5. would be very small and then the system would become sensitive only to the out-of-plane displacement gradient component. In this case, the Eq 4. reduces to:

$$\frac{\partial w}{\partial x} = \frac{\lambda \Delta_x}{4\pi \delta x} \quad (6)$$

And for shear in y direction:

$$\frac{\partial w}{\partial x} = \frac{\lambda \Delta_y}{4\pi \delta y} \quad (7)$$

Hence the out of plane components ∂w/∂x or ∂w/∂y can be measured.

Phase Calculation: Shearography fringe patterns calculated by Eq 3. are strongly affected by noise term $\sin(\varphi + \frac{\Delta}{2})$. Moreover subtraction of two speckle patterns, results in an intensity-based fringe pattern that does not provide the phase information leading to the need for quantative measurements. For the enhancement of fringe visibility, there are 2 main methods; phase map calculation and applying filtering algorithms.

The most common methods used to retrieve the phase map from fringe patterns are temporal phase shifting [21] and the Fourier transform method [22]. In the Temporal phase shifting method, a series of images (almost 4) are recorded with a known phase step between them. These images are then recombined using a phase-stepping algorithm [21] producing a wrapped phase map. In a Michelson-based shearing interferometer, phase shifting can be incorporated by mounting the reference mirror of Fig 1. on a piezoelectric transducer (PZT) which is used to shift the phase within the interferometer and enable temporal phase stepping. The commonly used phase stepping algorithms are the three, four and five-step algorithms [6]. Three-step algorithm is the fastest of them since only three fringe patterns with a relative phase of $2\pi/3$ between them are required. These fringe patterns can be combined using the three-step algorithm [6]:

$$\varphi = \tan^{-1}\left(\sqrt{3}\frac{I_3 - I_1}{2I_2 - I_1 - I_3}\right) \quad (8)$$

The resulted map, indicates a wrapped phase map where the pixel values are bound between-π and $+\pi$. This wrapped phase map is used for both crack detection and quantative measurement of the displacement derivatives of the surface.

Experimental Investigations

Specimen Preparation: Crack-type defects were simulated by cutting several grooves with same depth but different sizes as shown in Fig 2. There was no visible indication of the presence of the cracks on the opposite surface, which was the investigated side. In particular, test specimens were manufactured from an 8-layer quasi-isotropic fiber reinforced composite plate, with the following stacking sequence (0, +45,-45, 90)s with total thickness equal to 4.5mm. Mechanical properties of the components of the composite plates are shown in Table 1.

In the first test specimen, five Cracks (grooves) of different lengths (L) all have the same depth of 0.5mm and width of 0.2 mm were cut in two plates with total dimensions of 100x70x4.5mm as shown in Fig 2-a. Here the depth of defects is defined as the distance between the object surface and the defect boundary. For a surface breaking volumetric flaw (referred to as 'groove' in the following), this is the distance between the bottom of the groove and the object surface.

Fig. 2: Composite laminates manufactured with several cut grooves. (a) Vertical cracks and (b) oblique cracks with different angles

Table 1: Mechanical properties of the composite used in the experiments

property	unit	fiber	matrix
Tensile Modulus	(*GPa*)	71.7	3.21
Shear Modulus	(*GPa*)	28.9	1.2
Density	(Kg/m^3)	2540	1200
Volume ratio	(%)	35	65

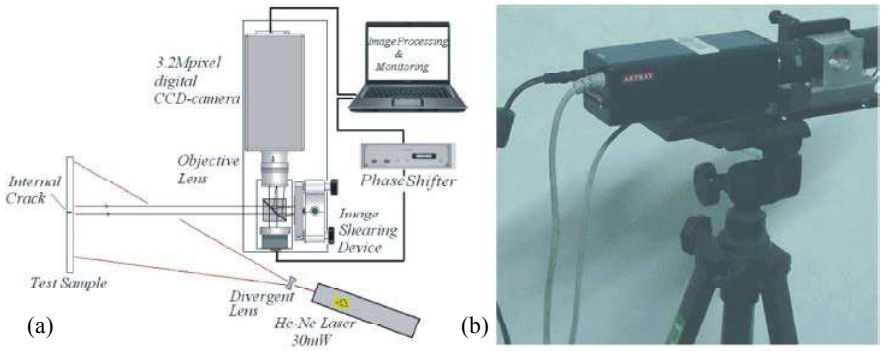

Fig. 3: (a) schematic of the shearography system used in this experiment (b) compact portable shearography head

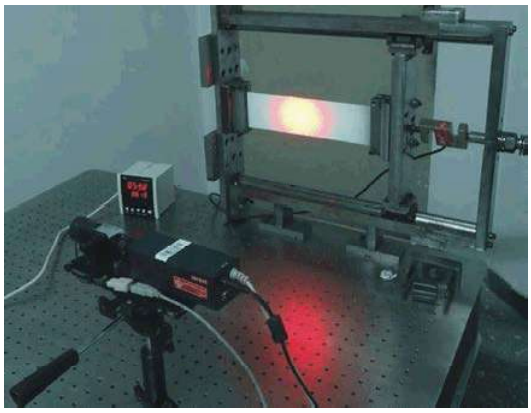

Fig. 4: Shearography test of defected objects using tensile loading system

The second specimen includes five cracks with the same length of 15mm, oriented in different angles as shown in Fig 2-b. The opposite surface (investigated side) of all the specimens was white painted to make them more reflective in the shearography test.

Experimental Procedure: A shearography system was set up according to Fig 3-a. This set-up consists of: a single wavelength (632.8nm) He-Ne laser tube and a beam expander used to illuminate the object; 3.2Mpixel digital CCD-camera and objective lens used to focus the image into the CCD-imaging target; Image-shearing device (here a modified Michelson interferometer) with phase shifter element (PZT); Image processing system and monitoring system. Shearing and capturing elements are compacted into a portable shearography head, designed and manufactured in the 'Intelligent Based Experimental Mechanics Center of Excellence, Tehran University' as shown in Fig 3-b.

The defected objects were subjected to the tensile loading by means of a loading system shown in Fig 4. Different amount of tensile loading and shearing distances were used in this investigation as shown in Table 2. for the tests of composite plates with defects of different size and orientation.

The speckle images reflected from the object surface is captured by the CCD camera through the image-shearing device. Two speckle patterns of the test object, before and after loading, are stored into the computer via the CCD-camera. The digital subtraction of these two speckle patterns will enable the reconstruction of a visible fringe pattern that depicts the displacement derivatives with respect to the direction of the shearing. All the observations were made from the front side of the test sample and the defects were on the back side. To obtain the phase map of the deformed shape, phase shifting procedure according to the algorithm mentioned in the part2 is applied. Image processing of the pictures include denoising and filtering were adopted to improve the fringe pattern quality.

Table 2: List of loading and shear amounts used in the tests

Test specimen	Defect length/inclination (mm/deg)	Loading amount (kgf)	Shear magnitude (mm)
Test plate no.1	L5/θ90	15,30,45,60,75,100	5,8
	L7.5/θ90	15,30,45,60,75	5,10
	L10/θ90		
	15,30,45,60,75,100	3,5,8,10,13	
Test plate no.2	L15/θ90	15,30,45,60,75,100	3,5,8,10,13
	L20/θ90		
	6,9.15,30,45,60,75	5,8,10	
Test plate no.3	L15/θ0	15,30,45,60,75,100	5,8,10,13
	L15/θ30		
	L15/θ60		
Test plate no.4	L15/θ15	15,30,45,60,75,100	5,8,10,13
	L15/θ45		
	L15/θ75		

RESULTS AND DISCUSSIONS

The visibility and quantification of the defects were achieved by evaluating the local concentration of fringes in the resulted shearograms achieved from mechanical loading of the specimens. The original fringe pattern (shearogram), filtered fringe pattern and relevant phase map of the L10mm crack of the test plate No. 1, tested with tensile load of 147N (15kgf) are shown in Fig 5. One of the main inherent drawbacks of the digital shearography testing is the low contrast of the fringe patterns and thus the defect testing accuracy. As it can be observed from the test images, the qualitative inspection of the object is better to be performed using phase map or filtered fringe pattern. Thus, the length of the crack can be approximated from the fringe anomalies and the defect depth can be calculated from the number of fringes around the defected zone. However, because the number of created fringes strongly related to the loading parameters, material properties and shearing distance, estimating the depth of the crack is much more complicated.

Here the shearing amount is set to 10mm in the x-direction, perpendicular to the loading direction and observation is set normal to the test surface.

The shearography results of the crack L10 in specimen no.1 excited by different tensile loads of 147N to 980N are shown in Fig. 6. In order to eliminate the effects of environmental conditions on the inspection results, all tests were performed with same parameters.

As it can be seen from the results, the minimum load that reveals the crack is around 150N. If the tensile loading exceeds 700N, fringes won't be visible more. Moreover the decorrelation effects caused by excessive loading will make the fringe patterns invisible, if the loading is not controlled in the inspection procedure.

The tests were performed in all the test plates with different loads and shearing distances according to Table 2. In each test the best matching load and shearing amount were obtained from the shearography results.

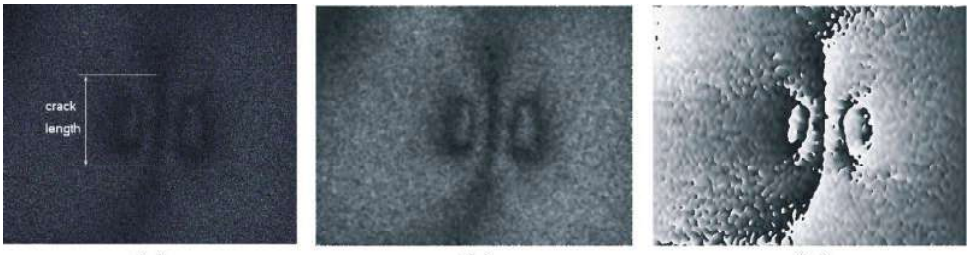

Fig. 5: Shearography test results of the L10mm crack with tensile loading of 147N a: shearogram, b: filtered shearogram, c: phase map

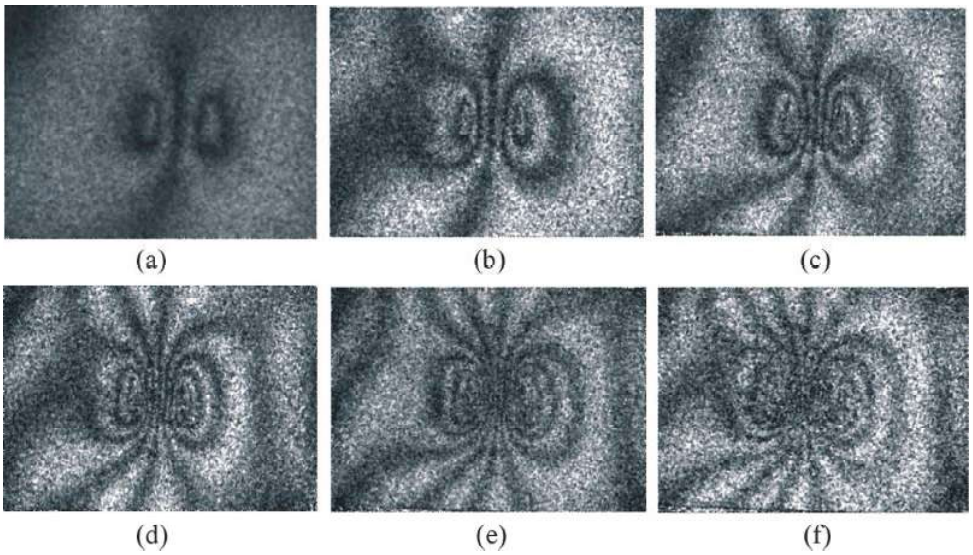

Fig. 6: Shearography test results of the L10mm crack with different loads, (a) 147N, (b) 294N, (c) 441N, (d) 588N, (e) 735N, (f) 980N

The main limitation of this method of testing is that the results are dependent on the physical geometry and dimensions of the specimens. So, the resulted load cannot be used for same cracks in other specimens. To overcome this problem, the loading should be dimensionless. So, in each case the average stress in the test plate in the cracked section was calculated and the ratio of stress over the tensile modulus of the material was defined as "load ratio" or "LR" which can be calculated from:

$$L.R = \frac{\sigma_{av}}{E_c} \tag{9}$$

where σ_w is the average stress in the test plate and E_c is the elasticity modulus of the composite plate.

Because shearography tests usually are performed in the elastic region of the material under test, the "LR" can be properly used as a dimensionless parameter to logically present the stress state needed for the inspection procedure. This parameter can be easily calculated from the geometry and loading status. Experiments show that "LR" is in the order of microns.

To calculate the "LR", the Young's modulus of the composite material is calculated from the Eq.10:

$$E_C = E_F V_F + E_M V_M \tag{10}$$

where E_c, E_F and E_M are composite, fiber and matrix Young's modulus, V_F and V_M are volume fraction of fiber and matrix respectively. So, for the test plates of this work:

$$E_C = 71.7 \times 0.35 + 3.21 \times 0.65 = 27 GPa$$

The lower limit of "LR" can be explained as the minimum load ratio that can be utilized to reveal a defect and the upper limit of "LR" as the maximum amount of applied load ratio that the fringe patterns are visible yet. Fig 7. shows selected shearography images from composite samples with different internal cracks, in which all the applied loads are the critical loads making lower limit of "LR" for the corresponding crack length.

Lower and upper limit of "LR" for all the cases obtained from the shearography tests are shown in Fig 8. A band region was therefore created that represents the critical ratios, which separates the detectable area and an undetectable one.

"LR" limits are related to the shearing distance in addition to the crack length. So, for each shearing distance, specific acceptable bounds of "LR" between lower and upper limits are obtained as shown in Fig 8. It means that for each crack length, if the "LR" set in the detectable area, the crack would be detected in the shearography inspection.

It can be seen from Fig 8. that for all of the cases, the amount of "LR" needed for the crack detection decreases as the crack length increases.

This trend can be used for selecting of a proper "LR" in an inspection procedure. For example in this case, if the shear distance in a shearography system set to 10mm, according to Fig 8-c, choosing the "LR" around 35e-6, makes the cracks with different lengths between 5mm to

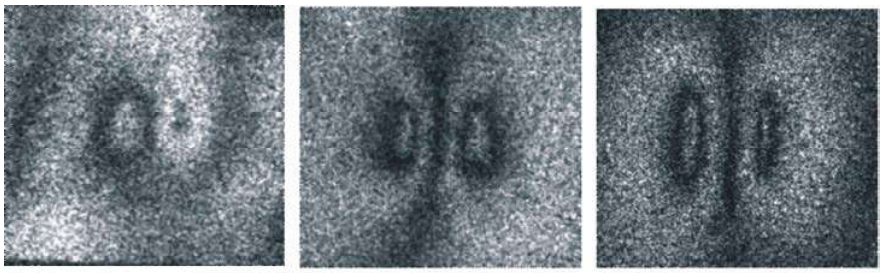

Fig. 7: Shearography fringe images for samples with internal cracks with critical load ratio: (a)L=5mm, LR=34µ, (b)L=10mm, LR=17µ, (c)L=20, LR=10.2µ.

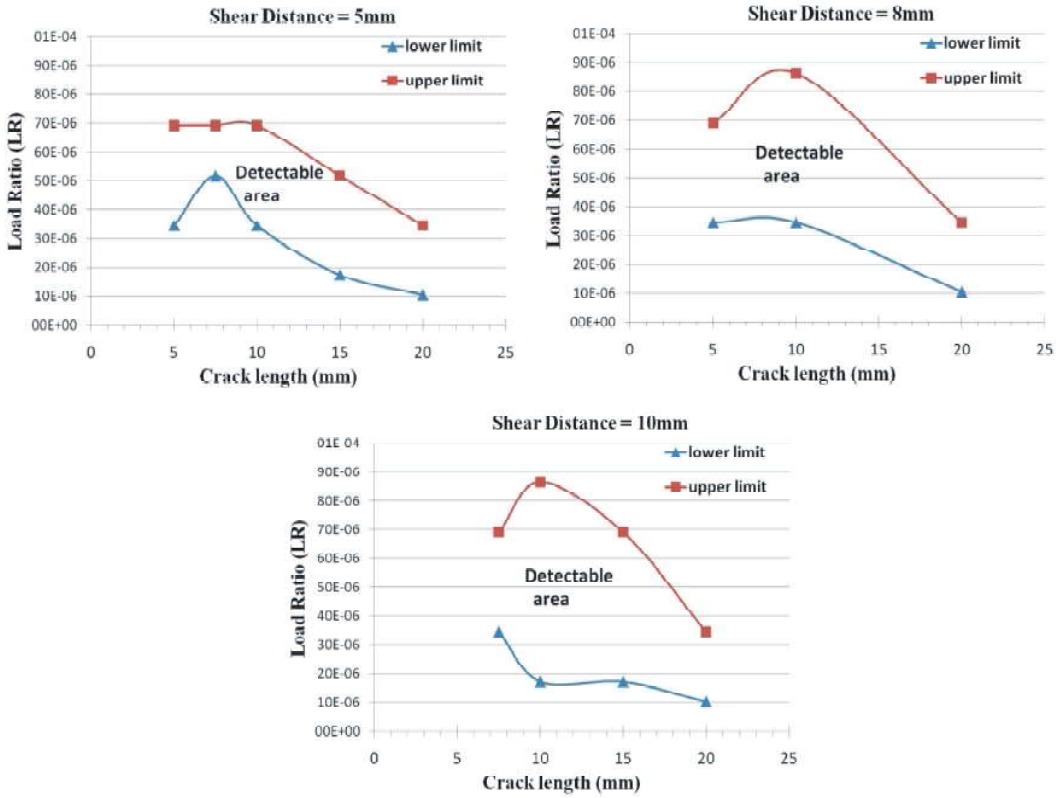

Fig. 8: Acceptable band of "LR" for detection of cracks with different lengths a) shear distance=5mm b) shear distance=8mm and c) shear distance=10mm

20mm detectable. However cracks with small lengths are more difficult to be recognized. Experiments show that the defect detection capability of shearography decreases rapidly when the size of the defect becomes smaller. This means that fringe disturbance caused by the crack is small and it is difficult to be recognized by the operator. On the other hand when the loading is very small, fringe disturbance becomes smaller. Since the background of a shearography image is speckle as Fig 8. shows, it is difficult to distinguish a relative small fringe disturbance against this speckle background. As a result, it is better to choose the amount of loading or "LR" in a middle band of the "LR" area. For example according to Fig 8-c for the crack length of 10mm, the best load ratio is around 50microns. This amount of load ratio is equivalent to the 441N resulting the fringe pattern of Fig 6-c.

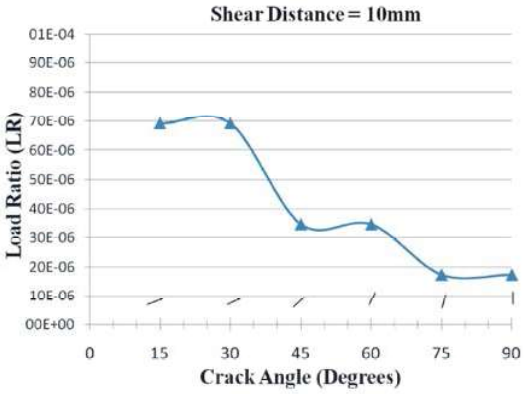

Fig. 9: The Load ratio "LR" for detection of cracks with different angles

Oblique Cracks: For the cracks with different orientations of test plates no.3 and 4, shearography test was performed with the parameters presented in Table 2. In all of the cases the best matching "LR" that leaded to a good quality fringe pattern was extracted and pointed in Fig 9. In the case of horizontal crack (θ=0) no visible fringe pattern was observed.

As it can be seen from Fig 9., as the inclination angle of the cracks with regard to the loading direction increases, the necessary loading required in the shearography test decreases. So, for detecting the inclined cracks, larger amounts of load ratio should be applied. On the other hand, larger "LR" may lower the fringe pattern quality due to the decorrelation effects; as a result, defects cannot be easily detected. Therefore, choosing a proper loading stage is an important step in the inspection procedure.

In the test plates discussed in the present paper, cracks with the lengths of 7.5 to 17.5 mm can be detected by applying the load ratio of around 40e-6 according to Fig 8-c; on the other hand, this amount of load ratio is enough for detection of cracks with the inclination angle of more than 45 degrees as Fig 9. shows. So, if the tensile loading is applied in two orthogonal directions, all the cracks will be detectable.

This procedure can be performed for different crack lengths, depths and different material to get curves of loading ratios that can be properly used in the inspection procedures.

To evaluate the sensitivity of the shearography system to the shearing direction, different shearing angles were applied during the inspection procedure. Evaluating the Results shows that when the orientation of the image shearing is parallel to the loading direction, the sensitivity for crack detection is relatively high compared with perpendicular or angular image shearing. So, it is concluded that in the procedure of crack detection, to get better results with relatively higher inspection sensitivity, it is better to choose the image shearing direction along the loading axis.

CONCLUSION

This paper presents a method to study the effects of mechanical loading parameters in the shearography test of fiber reinforced composites. An out of plane shearography set-up was adjusted and compacted to a portable head. Several test plates were prepared with deliberately made cracks, created with different sizes and orientations. Shearography NDT of the defected specimens was performed by applying different amounts of tensile loading. According to this study, the following conclusions can be made:

- In addition to disbound or delamination-type defects, internal cracks in the composite materials can be detected by an out of plane shearography system provided that a proper stress status is applied.
- Because in the shearography tests, the required amount of loading is almost in the elastic region of the material, the ratio of the elastic stress over the elastic modulus of the material can be properly used as a dimensionless practical measure for determining the loading status.
- For each crack length there is a range of acceptable load ratio that if the loading is lower or higher than it, the crack will not be visible in the shearography test. Knowing the acceptable range of "LR" leads to choose a proper stress status in the test procedure.
- For those defects having a larger ratio of length to width such as cracks and grooves, the shearography system is sensitive to the loading direction as well as shearing direction.
- When the loading and shearing directions are perpendicular to the crack direction, the crack length can be approximated from the fringe anomalies, but it becomes difficult to measure the borders of fringe anomalies when the shearing direction is not perpendicular to the crack direction.
- To improve the ability of crack detection of the shearography system, it is better to choose the image shearing direction along the loading axis.

Finally, it is envisaged that cracks in composite plates will become a defect type that can be detected and quantitatively characterized with confidence by digital shearography, in addition to delamination defects that are frequently being investigated in composite materials.

REFERENCES

1. Fotakis, C., D. Anglos, V. Zafiropulos, S. Georgiou and V. Tornari, 2006. Lasers in the preservation of cultural heritage. CRC Press.
2. Maldague, Z. and X. Maldague, 1993. Nondestructive Evaluation of Materials by Infrared Thermography, Springer.
3. Lokberg, O.J. and J.T. Malmo, 1988. Detection of defects in composite materials by TV holography, NDT International, 21: 223-228.
4. Edwards, C., I. Lira, A. Martinez and M. Miinzenrnayer, 2001. Electronic speckle pattern interferometry analysis of tensile tests of semihard copper sheets, Experimental Mechanics, 41: 58-62.
5. Hung, Y.Y., 1982. Shearography a new optical method for strain measurement and nondestructive testing, Optical Engineering, 21(3): 391-395.
6. Francis, D., R.P. Tatam and R.M. Groves1, 2010. Shearography technology and applications: a review, Measurement Science and Technology, 21: 1-29.
7. Hung, Y.Y., 1996. Shearography for non-destructive evaluation of composite structures, Optical Lasers Engineering, 24: 161-182.
8. Toh, S.L., F.S. Chau, V.P.W. Shim, C.J. Tay and H.M. Shang, 1990. Application of shearography in nondestructive testing of composite plates, Journal of Materials Processing Technology, 23: 267-275.
9. Garnier, C., M.L. Pastor, F. Eyma and B. Lorrain, 2011. The detection of aeronautical defects in situ on composite structures using Non Destructive Testing, Composite Structures, 93: 1328-1336.
10. DeAngelis, G., M. Meo, D.P. Almond, S.G. Pickering and S.L. Angioni, 2012. A new technique to detect defect size and depth in composite structures using digital shearography and unconstrained optimization, NDT and E International, 45: 91-96.
11. Liu, Z., J. Gao, H. Xie and P. Wallace, 2011. NDT capability of digital shearography for different materials, Optics and Lasers in Engineering, 49: 1462-1469.
12. Schöntag, J., D. Willemann and A.A. lbertazzi, 2010. Depth assessment of defects in composite plates combining shearography and vibration excitation, Optical Metrology Conference, pp: 7387.
13. Celine, F., A. Margarette and P. Almoro, 2012. Fringe analysis and enhanced characterization of sub-surface defects using fringe-shifted shearograms, Optics Communications, 285: 4223-4226.
14. Guo, G., J. Tu, Y. Zhang and Y. Shi, 2012. Inspection of Kissing-bond Defect in Honeycomb Structure by shearography, 18th World Conference on Nondestructive Testing, pp: 16-20.
15. Kim, G., S. Hong, G. Hee and K. Jhang, 2012. Evaluation of Subsurface Defects in Fiber Glass Composite Plate using Lock-in Technique, international journal of precision engineering and Manufacturing, 13: 465-470.
16. Malacara, D. and S. Mallick, 1976. Lateral shear interferometers. Applied Optics, 15: 2695-2697.
17. Zhang, C., B. Li, B. Zhao and X. Yuan, 2002. A static polarization imaging spectrometer based on a Savart polariscope, Optics Communications, 203: 21-26.
18. Murukeshan, V.M., O.L. Seng and A. Asundi, 1998. Polarization phase shifting shearography for optical metrological applications, Optics and Laser Technology, 30: 527-531.
19. He, Y.M., C.J. Tay and H.M. Shang, 1999. A new method for generating high visibility digital speckle shearing fringe pattern, Optik, 110(2): 86-88.
20. Schuth, M., F. Vössing and L. Yang, 2004. Shearographic Endoscope for Nondestructive Test, Journal of Holography and Speckle, 1: 46-52.
21. Yang, L.X., W. Steinchen, M. Schuth and G. Kupfer, 1995. Precision measurement and nondestructive testing by means of digital phase shifting speckle pattern and speckle shearing interferometry, Journal of the International Measurement Confederation, 16: 149-160.
22. Kaufmann, G.H., 2003. Phase measurement in temporal speckle pattern interferometry using the Fourier transform method with and without a temporal carrier, Optics Communications, 217: 141-149.